Applied Physics Letters

RESEARCH ARTICLE | NOVEMBER 02 2026

An STT-MTJ device operating below 4 K

Maximilian Sohr ; Christoph Durner ; Sina Ranjbar ; Meike Hindenberg ; Tatiana Gurieva ; Benjamin Lilienthal-Uhlig ; Sagar Gambhira ; Stuart S. P. Parkin ; Elena Hassinger ; Maximilian Lederer

Check for updates

Appl. Phys. Lett. 129, 182403 (2026)
https://doi.org/10.1063/5.0354254

View Online
Export Citation

Articles You May Be Interested In

Temperature-dependent analysis of retention and write characteristics of STT-MRAM cells

J. Appl. Phys. (November 2025)

10 November 2026 07:55:31



AIP Publishing

An STT-MTJ device operating below 4 K

Cite as: Appl. Phys. Lett. **129**, 182403 (2026); doi: 10.1063/5.0354254
Submitted: 28 July 2026 · Accepted: 19 October 2026 ·
Published Online: 2 November 2026

View Online Export Citation CrossMark

Maximilian Sohr,[1,a)] Christoph Durner,[1] Sina Ranjbar,[1] Meike Hindenberg,[1] Tatiana Gurieva,[1] Benjamin Lilienthal-Uhlig,[1] Sagar Gambhira,[2] Stuart S. P. Parkin,[2] Elena Hassinger,[3] and Maximilian Lederer[1]

AFFILIATIONS

[1]Center Nanoelectronic Technologies (CNT), Fraunhofer IPMS, 01109 Dresden, Germany
[2]Nano-Systems from Ions, Spins and Electrons (NISE), Max Planck Institute of Microstructure Physics, 06120 Halle (Saale), Germany
[3]Institute for Quantum Materials and Technologies, Karlsruhe Institute of Technology, 76131 Karlsruhe, Germany

[a)]**Author to whom correspondence should be addressed:** maximilian.sohr@fraunhofer.ipms.de

ABSTRACT

We report the cryogenic characterization of an out-of-plane anisotropy magnetic tunnel junction with an electrical Critical Diameter of 192 nm over measured sample-stage (nominal) temperatures from 2 to 300 K using spin-transfer torque (STT) switching. Even in the low-temperature limit, the critical switching current density remains below 4 MA/cm^2. After determining the magnetic properties of the film stack, we performed device-level measurements using magnetic-field and DC write-current sweeps. The tunnel magnetoresistance decreases approximately linearly with nominal temperatures, from 203% to 119%. The critical STT switching voltage remains nearly constant (<0.6 V) below 50 K and decreases monotonically at higher nominal temperatures, underscoring the suitability of STT magnetoresistive random-access memory for cryogenic memory applications. The free layer (FL) temperature during switching was estimated using finite-element simulations, which indicate that Joule heating can increase the device temperature by up to 120 K. Under the assumption of linearly extrapolated thermal conductivities, the critical switching voltage exhibits an approximately linear dependence on the FL temperature, in good agreement with the macrospin model. For a 400 ns program-erase cycle at 2 K, the mean dissipated power of the investigated device is 0.14 mW, indicating that the current density must be further reduced to enable large-scale array operation within realistic thermal budgets.

© 2026 Author(s). All article content, except where otherwise noted, is licensed under a Creative Commons Attribution (CC BY) license (https://creativecommons.org/licenses/by/4.0/). https://doi.org/10.1063/5.0354254

10 November 2026 07:55:31

Spin-transfer torque magnetoresistive random-access memory (STT-MRAM) is a promising emerging memory candidate due to its non-volatility, low energy dissipation, high endurance, scalability to sub-20 nm technology nodes, CMOS compatibility, and high speed.[1] It entered mass production in 2019 as an embedded non-volatile memory technology and successor to embedded flash memory.[2] As superconducting quantum computers scale, the thermal load from interconnects that connect the quantum processor to external memory becomes prohibitive, necessitating cryogenic memory that can interface with conventional logic at temperatures below 4 K. However, the power demand of existing memories such as DRAM is too high at 4 K.[3] Superconducting memories seem like a natural choice given their fast, ultra-low-loss operation, but they are hindered by large micrometer-scale circuits and poor energy efficiency at scale.[4] Another candidate is a three-terminal magnetic tunnel junction (MTJ) device that uses spin–orbit torque (SOT) for writing and is not limited by the MgO breakdown voltage. Although SOT switching down to 5 K has been demonstrated, e.g., in a heterogeneous van der Waals structure,[5] SOT switching of MTJ devices at cryogenic temperatures has only been shown in simulations.[6] STT-MRAM, on the other hand, has the advantage of being extensively studied and offers high storage capacity for a small footprint. Perpendicular MTJs have shown reliable nanosecond-pulse switching even at nominal temperatures as low as 2 K,[7] with a minimum switching energy of 103 fJ (286 fJ) into the parallel (P) [anti-parallel (AP)] state for devices with 40 nm diameter and higher switching energies for larger devices.[8] The dependency of the switching voltage on the temperature has been examined,[9] including effective junction temperature estimations.[10] The influence of the magnetic anisotropy of MTJs under cryogenic conditions has been characterized.[11,12] Double-barrier MTJs have shown to further decrease energy consumption.[13]

In this work, we present magnetometer measurements of a single barrier MTJ thin film stack from which a device with an electrical Critical Diameter (eCD) of 192 nm was fabricated and characterized

© Author(s) 2026

against field and STT current, demonstrating switching down to nominally 2 K with a current density of 1.0 MA/cm^2 (3.8 MA/cm^2) for switching into the parallel (anti-parallel) state. We then estimated the temperature of the free layer (FL) during operation after correcting for Joule heating using finite element method (FEM) simulations.

The MTJ thin film stack was deposited onto a 300 mm thermally oxidized Si wafer using DC and RF magnetron sputtering and annealed at 300 °C for 10 min. The stack structure is shown schematically in Fig. 1(a). The MTJ is formed by a free layer (FL) of $Co_{20}Fe_{60}B_{20}$ (1.6 nm), a tunnel barrier (TB) of MgO (1 nm), and a reference layer (RL) of $Co_{20}Fe_{60}B_{20}$ (1.2 nm). The RL is pinned by a synthetic antiferromagnet (SAF) consisting of two Co/Pt multilayers that are antiferromagnetically coupled with a thin Ru layer. The stack was chosen for its low coercivity at room temperature (RT) while exhibiting out-of-plane magnetic anisotropy in all ferromagnetic layers. Current-in-plane tunneling (CIPT) measurements were used to determine the tunnel magnetoresistance (TMR) at the film level at RT. A square 3.5 × 3.5 mm^2 sample from the thin film stack was measured in a superconducting quantum interference device magnetometer in vibrating-sample mode (SQUID-VSM) over a temperature range from 2 to 300 K. After magnetic and electrical characterization at the film level, circular devices with critical diameters ranging from 100 nm to 2 μm were fabricated using electron-beam lithography, ion-beam etching, and lift-off. The bottom electrode (BE) was defined first, followed by the preparation of the vias and nano-pillars. In the final step, Pt contact pads were added. Electrical measurements of the devices were performed under different magnetic fields and DC voltages in an OptiCool closed-cycle cryostat at sample-stage temperatures down to 2 K. We refer to the sample-stage temperature measured by the sensor marked with (4) in Fig. 2(c) simply as the

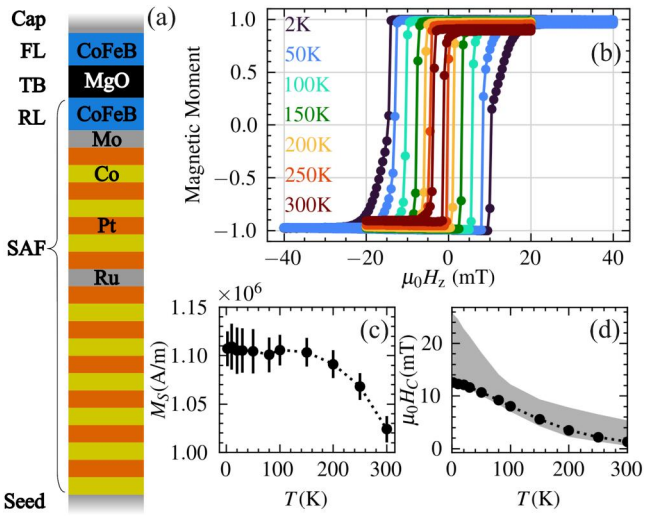


FIG. 1. (a) Schematic MTJ stack and (b) SQUID-VSM measurements of the film sample for different temperatures: The magnetic moment, normalized to saturated moment at 2 K, is plotted against the out-of-plane field, showing FL transitions. (c) Saturation magnetization M_S of the FL against temperature. Error bars are extracted from the difference between the start and end of the hysteresis loop. (d) Coercivity H_C derived from the zero-crossing of $M(H)$. The area between smallest and largest H_C, i.e., using inner and outermost transition, respectively, is shaded in gray.

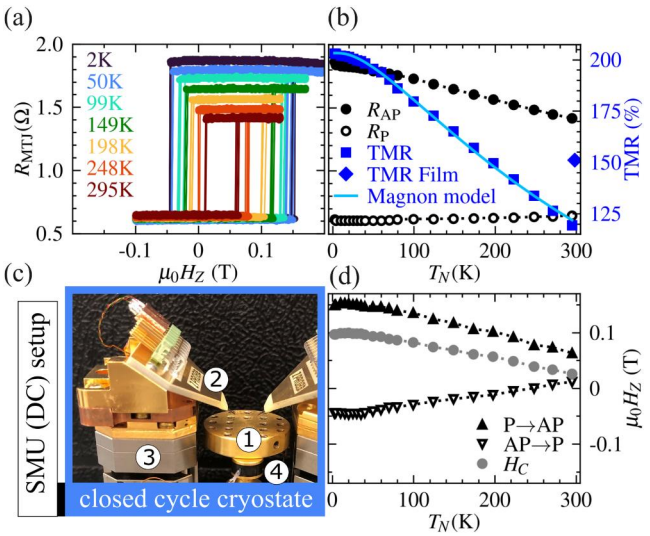


FIG. 2. Resistance vs field measurements of the nanopillar MTJ device with a read current of 10 μA. (a) Measured two-point resistance against the out-of-plane magnetic field for different nominal temperatures featuring five cycles each. (b) Extracted (anti-)parallel resistance R_P (R_{AP}) and derived tunnel magnetoresistance (TMR) with the TMR film value at room temperature obtained by CIPT. (c) Measurement setup with (1) a sample stage, (2) a needle card, (3) a movable Piezo tower, and (4) a temperature sensor. (d) Switching fields between parallel (P) and anti-parallel (AP) states with coercive field H_C.

nominal temperature T_N. A piezo-controlled probe setup was used for *in situ* electrical contacting, as shown in Fig. 2(c). All device measurements shown here were conducted during a single measurement campaign without recontacting and on the same device. Furthermore, we reproduced the measurement and found devices on the same coupon with slightly larger eCDs that showed similar TMR(T), $V_{AP\to P}(T)$, and $V_{P\to AP}(T)$ behavior. A positive voltage is defined as a positive potential applied to the BE, i.e., electrons tunnel from the FL to the RL, thereby causing or assisting the transition from the parallel (P) state to the anti-parallel (AP) state.

The thin film $M(H)$ behavior obtained by a SQUID-VSM is shown in Fig. 1(b) for different temperatures and demonstrates switching of the FL under out-of-plane magnetic field. The data are corrected for the background signal (the substrate and the sample holder). Note that a small offset field is present. We attribute this foremost to dipolar coupling from the SAF,[14] following the simulation of the magnetic field. At the lateral edges of the FL, the magnetic field from the top part of the SAF is pulling the FL magnetization in the same direction. In the center, the field from the larger bottom part of the SAF dominates the FL magnetization. In the film measurement [Fig. 1(a)], this leads to a negative offset field originating from the bottom SAF. In the device measurement [Fig. 2(a)], this results in a positive offset field in the much smaller MTJ device, because it has a higher edge to area ratio. Other influences such as exchange coupling and "orange peel" coupling between the RL and FL cannot be excluded; however, they would result in an offset field of the same sign, independent of the device or the film (size), and are, therefore, not the main reason for the offset field. The saturated moment was extracted for each temperature, divided by the FL volume, and plotted

10 November 2026 07:55:31

© Author(s) 2026

as the saturation magnetization M_S in Fig. 1(c). M_S increases with decreasing temperature and then reaches a plateau below 100 K. Figure 1(d) shows the coercivity H_C, determined as half the distance between the zero crossings of the hysteresis loops. Rather than exhibiting a single sharp switching field, the hysteresis loops display a transition region, which broadens significantly at low temperatures. Accordingly, the gray shaded area shows the region between the minimum and maximum values of H_C that can be extracted. Both quantities show a strong increase with decreasing temperature, meaning that larger fields are needed at low temperatures to reverse the magnetization of the FL. Domain-wall pinning is known to increase strongly at low temperatures,[15] which explains the stepped transitions, corresponding to states between the saturated regions in which some domains of the FL are magnetized along $+z$ and others along $-z$.

Figure 2(a) shows the nanopillar MTJ device switching between the measured P and AP resistance states, R_P and R_{AP}, respectively. The measurement started at a nominal temperature of 2 K and continued up to 300 K, with 5 cycles per temperature and 22 temperature steps. R_{AP} decreases with increasing nominal temperatures [see Fig. 2(b)]. Meanwhile, R_P shows a very small increase of approximately 5% (40 Ω) with nominal temperatures, contrary to other reports.[16] A possible explanation is temperature-dependent mechanical stress on the probe needles, affecting the contact resistance. Assuming that $\mathrm{TMR}_{\mathrm{film}} = \mathrm{TMR}_{\mathrm{device}}$ yields a parasitic serial resistance of $R_C = 138\,\Omega$ at 300 K and an eCD of 192 nm. The temperature dependency of the TMR is caused by R_{AP} and can be well fitted using the magnon excitation model,[17,18]

$$\mathrm{TMR}(T) = \frac{\mathrm{TMR}(0)+1}{1-2Q\beta_{\mathrm{AP}}\ln(1-\exp(-E_C/k_BT))} - 1, \qquad (1)$$

where Q is the probability for a magnon involved in the tunneling process, E_C is the magnon cutoff energy, $\beta_{\mathrm{AP}} = Sk_BT/E_m$ with the spin parameter $S = 3/2$, and $E_m = 3k_BT_C/(S+1)$ with the Curie temperature T_C of the RL and the FL. From film measurements [Fig. 1(c)], we estimate the Curie temperature of our FL to 650 K and fix TMR(0) to the measured 2 K value. This gives us $Q = 0.26$ and $E_C = 3.0$ meV, which is in the typical range of reported literature values.[16,19] The relatively high magnon probability indicates a significant contribution of incoherent tunneling. Figure 2(d) shows the switching fields and the coercive field H_C, which both saturate below 50 K. This can be in part explained by the measured $H_C(T)$ on the film level [Fig. 1(d)]. It should be noted that according to all FEM simulation scenarios, explained later in the text, we do not expect relevant Joule heating from the 10 μA read current.

To demonstrate operation of the memory cell, we swept the nanopillar MTJ device using write voltages up to 0.8 V with 50 cycles at each nominal temperature. The 10 ms write pulses (the DC regime) were each followed by 10 ms read pulses of 10 mV. R_{MTJ} in Fig. 3(a) was calculated from the write pulses and exhibits the known house-shape characteristic, which can be attributed to the non-linear $R_{\mathrm{MTJ}}(V)$. STT switching was only possible for $T_N < 250$ K, because, at higher nominal temperatures, the FL is no longer bi-stable owing to the offset field from the SAF and the low H_C. Figure 3(b) shows the evolution of the switching voltage and current density as a function of the nominal temperature. The switching voltage $V_{\mathrm{AP}\to\mathrm{P}}$ is generally lower than $V_{\mathrm{P}\to\mathrm{AP}}$. This can be attributed primarily to the offset field[14] of approximately 50 mT (see Fig. 2) that favors the P state and

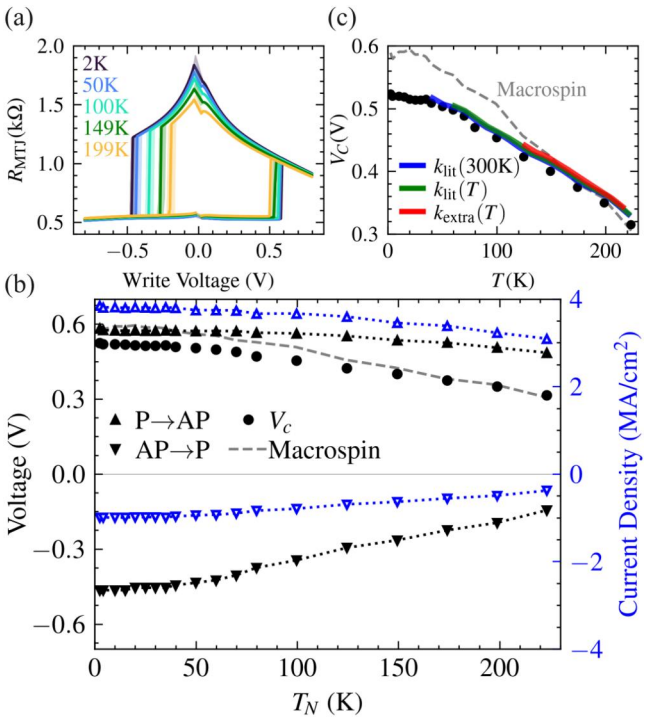


FIG. 3. Measurement results of the write voltage sweep of the nanopillar MTJ device. (a) 49 cycles per nominal temperature step (semi-transparent) and median resistance (solid lines). (b) Extracted switching voltages (left axis, black and gray) between parallel (P) and anti-parallel (AP) states with coercive voltage V_C against the nominal temperature. The right axis shows, in blue, the switching current densities assuming the calculated eCD. Critical switching voltage from the macrospin model [Eq. (2)] as the dashed gray line in (b) and (c). (c) Measured V_C (black) and temperature-corrected V_C (colored) vs temperature.

secondly to the higher STT efficiency for AP → P. Furthermore, $V_{\mathrm{AP}\to\mathrm{P}}$ shows a stronger nominal temperature dependence, which is due to $R_{\mathrm{AP}} > R_{\mathrm{P}}$. The current densities for AP → P and P → AP increase similarly in absolute values. Like $H_C(T)$ in Fig. 2(d), we see a flattening in $V_C(T)$ around 50 K. According to the macrospin model, the critical switching voltage for a symmetric junction is given by[20]

$$V_C(T) = \alpha\frac{2e}{\hbar}\left(\frac{1+P(T)^2}{P(T)}\right)\mu_0 H_{k,\mathrm{eff}}(T)\mu(T)R_P, \qquad (2)$$

where α is the damping parameter, e is the electron elementary charge, $\hbar$ is the reduced Planck's constant, μ_0 is the permeability of free space, $H_{k,\mathrm{eff}}$ is the effective perpendicular anisotropy field, and μ is the magnetic moment. For simplicity, the spin polarizations of the RL and the FL are assumed to be equal, i.e., $P_{\mathrm{RL}} = P_{\mathrm{FL}} = P$. Assuming $H_{k,\mathrm{eff}} = 2H_C$[21] and $\alpha(T) = 0.02$,[10] we obtain the dashed lines in Figs. 3(b) and 3(c). The predicted $V_C(T)$ is dominated by the estimated $H_{k,\mathrm{eff}}$ factor and subsequently shows a similar flattening at low temperatures as $H_C(T)$. The discrepancy below 120 K can be primarily explained by Joule heating, which is discussed below.

It is experimentally challenging to determine the FL temperature of the MTJ during operation. This is because the tunnel resistance of the MTJ depends on both temperature and the applied voltage.

10 November 2026 07:55:31

© Author(s) 2026

The applied voltage, in turn, is the source of the Joule heating. Similarly, the switching field is influenced by both the read voltage (via STT assist) and the temperature. FEM simulations offer a way to get a plausible estimate. The results shown in this work were obtained using the software COMSOL Multiphysics. However, it is very difficult to accurately estimate the effective thermal conductivities $k(T)$ for many atomically thin layers in the stack, especially for different temperatures. We approached this by dividing the simulation into three scenarios from conservative to simple best-guess assumptions, differing in the used $k(T)$:

1. Use values at 300 K, independent of present temperature. Thin film values from literature were used where available; otherwise, bulk values were used.
2. As in scenario 1, but using temperature-dependent values where available; otherwise, the closest available value was used.
3. Linear extrapolation down to 2 K based on literature values and the Wiedemann–Franz law.

Since DC voltages were used, i.e., the steady state regime, variations in heat capacity do not affect the converged simulation result. From electromagnetic heating simulations, the TB was identified as the main heat source. Therefore, we used a pure heat transfer simulation with $P_{\text{heating}} = R \cdot I^2$ within the MgO volume.

Figure 4(b) shows the result for a nominal temperature of 2 K, an experimentally measured switching current $I_{P\rightarrow AP} \approx 1.1$ mA and $R_P \approx 387\,\Omega$ for scenario 1. The white contour lines and labels indicate the structure of the nanopillar MTJ device, adapted from a TEM image of a similar device. Significant heating is observed even in the conservative scenario resulting in a mean FL temperature of 40 K. The top electrode surface, which is insulated by a vacuum, and the edge of the pillar, which is encapsulated by aluminum oxide, cause heat to accumulate. The resulting mean FL temperatures for all three scenarios, evaluated at all measured nominal temperatures and their corresponding (measured) switching currents, are plotted in Fig. 4(a). Since the switching current (quadratic term in P_{heating}) into the AP state is much larger, the heating is also substantially higher for the P → AP direction (dashed) for all scenarios, even though $R_P < R_{AP}$. Another striking difference is observed between the extrapolated scenario (red) and the other two scenarios. The former predicts heating up to 120 K, accounting for the strong thermal boundary resistance at low temperatures. Figures 4(c) and 4(d) show the measured switching currents and the same data shifted in temperature according to the three scenarios. The extrapolated scenario results, then, in a linear relation of the switching current vs the FL temperature. In Fig. 3(c), the temperature-corrected coercive voltage curves are compared with the macrospin model prediction. Here, the extrapolated scenario demonstrates the best agreement with the theoretical model.

In summary, we characterized an out-of-plane anisotropy nanopillar MTJ device with an eCD of 192 nm over nominal temperatures ranging from 2 K to RT. We first examined the magnetic properties of the film, then proceeded to device measurements using magnetic-field sweeps and DC write-current sweeps, and finally estimated the FL temperature during the switching process using FEM simulations to model Joule heating. The TMR is observed to decrease with increasing the nominal temperature and can be adequately described by the magnon excitation model. This model attributes the temperature dependence to incoherent tunneling. The critical switching

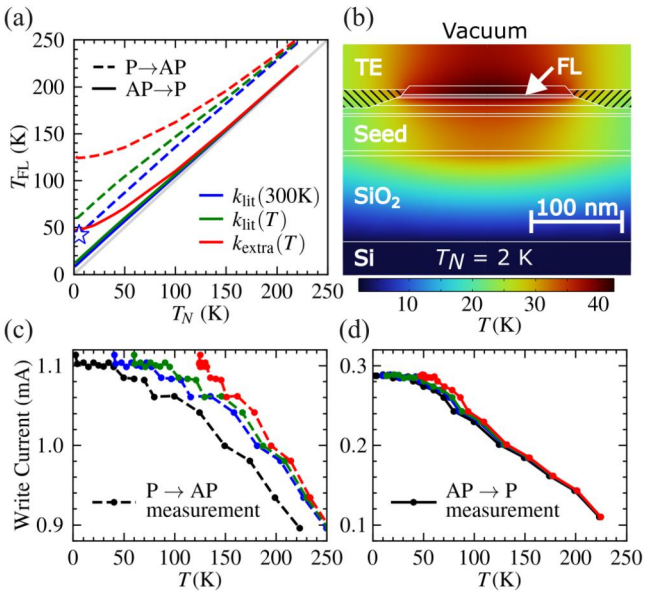


FIG. 4. Results of FEM simulations of Joule heating in the nanopillar MTJ device with the tunnel barrier (MgO) as a heat source. (a) Mean temperature T_{FL} of the FL for different set nominal temperatures T_N and different thermal conductivities: assuming 300 K (blue), literature values where available (green), and extrapolated values (red). The experimentally determined P → AP and AP → P switching currents were used for the simulation, yielding the dashed and solid lines, respectively. (b) Cross section of the simulated nanopillar MTJ device. The edges of the layers are marked in white, with the Pt top electrode (TE), Al_2O_3 encapsulation (black hatched), a free layer (FL), seed layers, and a substrate (SiO_2 and Si). The plot shows the P → AP transition at a nominal temperature of $T_{nominal} = 2$ K for constant thermal conductivities from the literature [the blue star in (a)]. Measured switching currents are shown in black for (c) P → AP and (d) AP → P vs the set nominal temperature. The colored points show the estimated FL temperatures according to the three scenarios drawn in (a).

current and voltage remain nearly constant below 50 K and decrease steadily with increasing the nominal temperature. FEM simulations of Joule heating using extrapolated thermal conductivities yield a linear trend for the critical switching current as a function of the FL temperature. The critical switching current density remains below 4 MA/cm^2 even at a nominal temperature of 2 K. In industrial grade devices, one typically uses write pulses on the order of 100 ns,[22] which are still in the thermal switching regime and translate into only slightly higher switching voltages at cryogenic temperatures than the DC voltages used in our measurement.[9] In the following, we assume $V_{STT}(100\,\text{ns}) \approx V_{STT}(\text{DC})$. If 7000 of these MTJ devices were operated in parallel in a program-erase cycle, i.e., write1–wait–write0–wait, with 100 ns per step and at 2 K, it would amount to approximately 1 W of mean heating power under continuous operation. We note that for the power calculation of the AP → P switch, one must consider the AP tunnel resistance at the applied voltage, which is significantly lower than R_{AP} measured at a small read voltage. Furthermore, our calculations include a parasitic contact resistance of 138 Ω derived from room temperature, which could lead to a slight overestimate of heating power. The heating power estimation highlights the importance of further reducing the current density in order to achieve scalable systems. Since the thermal stability of the FL increases at

10 November 2026 07:55:31

© Author(s) 2026

cryogenic temperatures, the magnetic anisotropy can be chosen lower as for room temperature MTJs to decrease the switching voltage.[12] Rehm *et al.* showed switching with sub-ns pulses at 4 K, which increases the voltage, but it requires overall less switching energy. Furthermore, the switching energy decreases for a smaller eCD.[8] Double tunnel barrier MTJs (DMTJs) have been shown to reduce current densities by more than double at room temperature and at 77 K.[23] Voltage-controlled magnetic anisotropy (VCMA) devices[24,25] promise switching with only minimal currents flowing, thereby diminishing Joule heating.

This study was supported by the Fraunhofer–Max Planck cooperation program in the Joint Initiative for Research and Innovation (*Pakt für Forschung und Innovation*/project *CONDOR*).

AUTHOR DECLARATIONS

Conflict of Interest

The authors have no conflicts to disclose.

Author Contributions

Maximilian Sohr: Conceptualization (equal); Data curation (lead); Formal analysis (lead); Investigation (lead); Methodology (equal); Software (lead); Visualization (lead); Writing – original draft (lead). **Christoph Durner:** Conceptualization (equal); Methodology (equal); Writing – review & editing (equal). **Sina Ranjbar:** Conceptualization (equal); Writing – original draft (supporting); Writing – review & editing (equal). **Meike Hindenberg:** Conceptualization (equal); Methodology (equal); Writing – review & editing (equal). **Tatiana Gurieva:** Conceptualization (equal); Methodology (equal); Writing – review & editing (equal). **Benjamin Lilienthal-Uhlig:** Conceptualization (equal); Funding acquisition (equal); Methodology (equal); Project administration (lead); Supervision (equal). **Sagar Gambhira:** Investigation (equal). **Stuart S. P. Parkin:** Funding acquisition (equal); Project administration (equal); Supervision (equal). **Elena Hassinger:** Supervision (equal). **Maximilian Lederer:** Conceptualization (equal); Methodology (equal); Supervision (equal); Writing – review & editing (equal).

DATA AVAILABILITY

The data that support the findings of this study are available from the corresponding author upon reasonable request.

REFERENCES

[1]T. Na, S. H. Kang, and S.-O. Jung, "STT-MRAM sensing: A review," IEEE Trans. Circuits Syst. II **68**, 12–18 (2021).
[2]See https://news.samsung.com/global/samsung-electronics-starts-commercial-shipment-of-emram-product-based-on-28 nm-fd-soi-process for "Samsung Electronics Starts Commercial Shipment of eMRAM Product Based on 28 nm FD-SOI Process" (2019).
[3]F. Ware, L. Gopalakrishnan, E. Linstadt, S. A. McKee, T. Vogelsang, K. L. Wright, C. Hampel, and G. Bronner, "Do superconducting processors really need cryogenic memories?," in *Proceedings of the International Symposium on Memory Systems*, edited by B. Jacob (ACM, New York, NY, 2017), pp. 183–188.
[4]S. Alam, M. S. Hossain, S. R. Srinivasa, and A. Aziz, "Cryogenic memory technologies," Nat. Electron. **6**, 185–198 (2023).
[5]O. Iqbal, Z. Muhammad, W. Ali, F. Wang, M. S. Hossain, A. Rahman, S. S. Alarfaji, Y. Zhang, X. Lin, M. Z. Hasan *et al.*, "Temperature-robust exchange bias and spin-orbit torque switching in van der Waals heterostructure," InfoMat **8**, e70064 (2026).
[6]J. Park, G. Rowlands, O. Lee, D. Ralph, and R. Buhrman, "Macrospin modeling of sub-ns pulse switching of perpendicularly magnetized free layer via spin-orbit torques for cryogenic memory applications," Appl. Phys. Lett. **105**, 102404 (2014).
[7]D. Lyu, P. Khanal, Y. Lv, B. Zhou, H. Yun, Q. Jia, B. R. Zink, Y. Fan, K. A. Mkhoyan, W. Wang, and J.-P. Wang, "Sub-ns switching and cryogenic-temperature performance of Mo-based perpendicular magnetic tunnel junctions," IEEE Electron Device Lett. **43**, 1215–1218 (2022).
[8]L. Rehm, G. Wolf, B. Kardasz, M. Pinarbasi, and A. D. Kent, "Sub-nanosecond spin-torque switching of perpendicular magnetic tunnel junction nanopillars at cryogenic temperatures," Appl. Phys. Lett. **115**, 182404 (2019).
[9]L. Lang, Y. Jiang, F. Lu, C. Wang, Y. Chen, A. D. Kent, and L. Ye, "A low temperature functioning CoFeB/MgO-based perpendicular magnetic tunnel junction for cryogenic nonvolatile random access memory," Appl. Phys. Lett. **116**, 022409 (2020).
[10]L. Rehm, G. Wolf, B. Kardasz, E. Cogulu, Y. Chen, M. Pinarbasi, and A. D. Kent, "Thermal effects in spin-torque switching of perpendicular magnetic tunnel junctions at cryogenic temperatures," Phys. Rev. Appl. **15**, 034088 (2021).
[11]P. B. Veiga, A. Mora-Hernandez, M. Dammak, S. Auffret, I. Joumard, L. Vila, L. D. Buda-Prejbeanu, I. L. Prejbeanu, B. Dieny, and R. C. Sousa, "Control of interface anisotropy for spin transfer torque in perpendicular magnetic tunnel junctions for cryogenic temperature operation," AIP Adv. **13**, 025253 (2023).
[12]S. Martín Rio, K. S. Senapati, L. Farcis, L. Soumah, P. B. Veiga, K. Garello, and R. C. Sousa, "Optimizing effective anisotropy in magnetic tunnel junctions for operation at cryogenic temperatures," Phys. Rev. Appl. **24**, 024016 (2025).
[13]E. Garzón, L. Yavits, A. Teman, and M. Lanuzza, "STT-MRAM technology for energy-efficient cryogenic memory applications," in *IEEE 14th Latin America Symposium on Circuits and Systems (LASCAS)* (IEEE, 2023).
[14]M. Hindenberg, A. Talapatra, B. Lilienthal-Uhlig, J. Müller, R. Hoffmann, and T. Mikolajick, "Offset field extraction with multi-bit magnetic tunnel junction structures," IEEE Trans. Electron Devices **72**, 3565–3572 (2025).
[15]G. Vértesy, I. Tomás, and Z. Vértesy, "On the temperature dependence of domain wall pinning field in soft, uniaxial magnetic materials," J. Phys. D **35**, 625–630 (2002).
[16]V. Drewello, J. Schmalhorst, A. Thomas, and G. Reiss, "Evidence for strong magnon contribution to the TMR temperature dependence in MgO based tunnel junctions," Phys. Rev. B **77**, 014440 (2008).
[17]Y. Wang, H. Cai, L. A. Naviner, Y. Zhang, J.-O. Klein, and W. Zhao, "Compact thermal modeling of spin transfer torque magnetic tunnel junction," Microelectron. Reliab. **55**, 1649–1653 (2015).
[18]S. Zhang, P. Levy, A. Marley, and S. Parkin, "Quenching of magnetoresistance by hot electrons in magnetic tunnel junctions," Phys. Rev. Lett. **79**, 3744 (1997).
[19]K. Cao, H. Li, W. Cai, J. Wei, L. Wang, Y. Hu, Q. Jiang, H. Cui, C. Zhao, and W. Zhao, "Low-temperature performance of nanoscale perpendicular magnetic tunnel junctions with double MgO-interface free layer," IEEE Trans. Magn. **55**, 1–4 (2019).
[20]B. Dieny and I. L. Prejbeanu, "Magnetic random-access memory," in *Introduction to Magnetic Random-Access Memory* (John Wiley & Sons Inc., 2017), pp. 101–164.
[21]C. Iglesias, J. De Araujo, E. Silva, M. Gamino, M. Correa, and F. Bohn, "Fundamental inequalities in the Stoner-Wohlfarth model," Phys. Rev. B **106**, 094405 (2022).
[22]S. Mangadahalli Siddaramu, M. Hindenberg, J. Müller, M. Wagner-Reetz, and J. Chatterjee, "Temperature-dependent analysis of retention and write characteristics of STT-MRAM cells," J. Appl. Phys. **138**, 203903 (2025).
[23]T. Moposita, E. Garzón, A. Teman, and M. Lanuzza, "Cryo-simply: A reliable STT-MRAM-based smart material implication architecture for in-memory computing," Nanomaterials **15**, 9 (2024).
[24]D. Favaro, W. Kim, S. Ranjbar, M. G. Monteiro, R. Carpenter, S. Rao, S. Van Beek, L. Labbate, J. Van Houdt, K. Temst *et al.*, "Switching of a magnetic tunnel junction by voltage-controlled magnetic anisotropy," Phys. Rev. Appl. **23**, 014040 (2025).
[25]P. B. Veiga, R. C. Sousa, L. D. Buda-Prejbeanu, S. Auffret, I. Joumard, L. Vila, I.-L. Prejbeanu, and B. Dieny, "Engineering of voltage-controlled magnetic anisotropy magnetic tunnel junctions at cryogenic temperatures," IEEE Trans. Magn. **59**, 1–5 (2023).

10 November 2026 07:55:31

© Author(s) 2026